Photochemical & Photobiological Sciences

The effects of solvent and micellar encapsulation on the photostability of avobenzone

Journal:	*Photochemical & Photobiological Sciences*
Manuscript ID	PP-ART-12-2019-000483.R1
Article Type:	Paper
Date Submitted by the Author:	31-Jan-2020
Complete List of Authors:	Hanson, Kerry; University of California Riverside, Chemistry Cutuli, Miles; University of California Riverside, Chemistry Rivas, Tiffany; University of California Riverside, Chemistry Antuna, Miranda; University of California Riverside, Chemistry Saoub, Jessica; University of California Riverside, Chemistry Tierce, Nathan; University of California Riverside, Chemistry Bardeen, Christopher; University of California Riverside, Chemistry

Effects of solvent and micellar encapsulation on the photostability of avobenzone

Kerry M. Hanson*, Miles Cutuli, Tiffany Rivas, Miranda Atuna, Jessica Saoub, Nathan T. Tierce and Christopher J. Bardeen*

Department of Chemistry
University of California, Riverside
501 Big Springs Road
Riverside, CA 92521 (USA)

*email: kerry.hanson@ucr.edu

*e-mail: christopher.bardeen@ucr.edu

Abstract

The photodegradation of avobenzone (**AV)**, the only ultraviolet filter molecule approved by the Food and Drug Administration to absorb UVA radiation, is an important problem in sunscreen formulations. In this paper, the photophysics and photostability of **AV** in various solvent systems and in aqueous micelles are studied. **AV** in its keto-enol tautomer functions as an effective UVA protection agent. **AV** is highly susceptible to photoinduced diketonization in both nonpolar solvents and in aqueous aggregates but is considerably more stable in polar, protic solvents like methanol. By studying its stability in different surfactant solutions, we show that incorporation of **AV** into sodium dodecylsulfate (SDS) micelles can achieve stability levels comparable to neat methanol. Steady- state spectral shifts, fluorescence anisotropy, and time-resolved fluorescence decay measurements are all consistent with **AV** experiencing a polar environment after micellar encapsulation. It is proposed that **AV** is encapsulated in the palisade layer of the SDS micelles, which allows access to water molecules that facilitate the re-formation of the enol form after photon absorption and relaxation. Although the detailed mechanism of **AV** tautomerization remains unclear, this work suggests that tuning the chemical microenvironment of **AV** may be a useful strategy for improving sunscreen efficacy.

Introduction

Photodamage of the skin results from the absorption of ultraviolet (UV) radiation by intrinsic chromophores found in both the epidermis and dermis. This damage includes immediate effects like erythema, melanogenesis, and immunodulation as well as delayed effects like photoaging, actinic keratosis, and carcinogenesis.[1-7] Sunscreens use UV filters to protect the skin either by scattering (physical sunscreens) or by absorbing (chemical sunscreens) UVB (280 nm – 320 nm) and UVA (320 nm – 450 nm) radiation before these photons can penetrate into the skin. Ideally, a chemical UV filter absorbs a photon and then quickly relaxes through nonradiative pathways, effectively converting the high energy UV photon into low energy vibrations or heat.[8-15] In addition, a UV filter should be stable and not undergo chemical changes that lessen its ability to absorb UV light or modify its toxicity. Today, the Food and Drug Administration (FDA) recognizes the importance of photostability in sunscreen function and requires a photochemical stability test as one of its criteria for sunscreen evaluation.[16]

Avobenzone (4-*tert*-butyl-4'-methoxydibenzoylmethane, (**AV**)) is a 1,3-dicarbonyl compound that is currently the only UVA-absorbing filter molecule approved by the FDA for use in sunscreens. It is also highly photolabile under UVA irradiation.[17-22] Avobenzone can exist in multiple isomeric forms, three of which are illustrated in Scheme 1: the intramolecular keto-enol chelate, the non-chelated keto-enol, and the diketone form.[23, 24] The most stable isomer is the keto-enol intramolecular chelate which exhibits a strong oscillator strength in the UVA created by a π-π^* transition due to conjugation through the carbonyl-ethylene unit.[20, 25, 26] This isomer is responsible for the UVA protection of **AV**. The more polar diketone isomer absorbs mainly in the UVC region (260 nm – 280 nm) and thus does not afford protection against UV photons that

reach Earth's surface.[12, 18, 20-22, 25, 27] Formation of the metastable diketone leads to two inter-related problems.[12, 18, 27] First, it no longer absorbs UVA due to loss of the conjugation across the keto-enol bridge, which in practical terms correlates to efficacy loss of avobenzone as a UVA absorbing sunscreen. Second, excitation of the n-π* transition of diketone **AV** generates a triplet state (500 ns, E_T=59.5 kcal mol^{-1}) that can sensitize singlet oxygen, as well as undergo a Norrish Type I reaction where the alpha-carbon splits forming two radicals, leading to complete photodegradation of **AV**.[17, 22, 28] Currently, the primary method for improving **AV** photostability, and thus its efficacy, relies upon enabling **AV** to undergo excited state energy transfer to a different molecule.[28, 29] A more general method to prevent **AV** isomerization to the diketone form would help preserve its UVA protection capability and improve sunscreen efficacy.

Currently, the mechanism of how **AV** partitions between the diketone and keto-enol tautomers after photoexcitation remains unclear. Upon excitation, the keto-enol chelate is broken, enabling rapid internal conversion back to the electronic ground state manifold, where it partitions between multiple non-chelated isomers.[30] These isomers can either relax back to the intramolecular chelated tautomer on longer timescales or undergo intramolecular hydrogen migration to form the diketone.[20, 30] This process appears to be solvent dependent, where tautomerization is detected in non-polar (cyclohexane, isooctane) and polar, aprotic (DMSO, acetonitrile) solvents but is effectively absent in polar, protic solvents like methanol.[20-22, 28, 31-35] Given the beneficial effects of this class of solvents, one might hope that water, a solvent that is known to effectively mediate proton transfer reactions, would have a stabilizing effect on **AV**. However, like other hydrophobic UV filters, **AV** is almost completely insoluble in H_2O. Recently, we found that the photostability of the UVB filter molecule octylmethoxycinnamate was strongly

reduced by aggregation in water.[36] In this paper, we examine how the local solvent environment affects **AV** photostability. We are particularly interested in controlling the access of H_2O molecules to **AV** using micellar encapsulation. The ultimate goal is to identify conditions that stabilize **AV** in its keto-enol tautomer where it can function as an effective UVA protection agent. The results in this paper show that tuning the chemical microenvironment of **AV** may be a useful strategy for improving sunscreen efficacy.

Experimental

Reagents. Avobenzone (98%) was provided by Merck Consumer Care Inc. (Memphis, TN). All solvents (cyclohexane, methanol, ethylene glycol, acetonitrile) and surfactants (cetrimonium bromide (CTAB), trimethylammonium bromide (TTAB), sodium dodecylbenzenesulfonate (SDBS), sodium laurate (SL), sodium dodecyl sulfate (SDS), >99%) were obtained from Sigma-Aldrich and used without further purification. MilliQ water was used for the surfactant solutions.

Sample Preparation. Photostability and fluorescence experiments in neat solvents were done using dilute solutions of **AV** (*ca.* 6 μM) in cyclohexane, methanol, ethylene glycol and acetonitrile. To create dry acetontitrile, anhydrous magnesium sulfate was added to 10 mL of 0.6 μM **AV**, and the solution was allowed to stand in the dark for 1 hr before the photostability tests were performed. To make suspensions of colloidal **AV** particles in water and surfactants (SDS, CTAB, TTAB, SDBS, SL) the re-precipitation method was used.[36] 200 μL of 10 mM **AV** in methanol was quickly injected into a rapidly stirred solution of 10 mL MilliQ water or surfactant (CTAB (2 mM)

, TTAB (8 mM), SDBS (5 mM), SL (42 mM), and SDS (2 mM, 4 mM, 6 mM, 8 mM, 10 mM, 12 mM, 15 mM and 20 mM)) . Each solution was stirred uncovered for 45 minutes to allow evaporation of the methanol. Subsequently, a 300 μL aliquot was transferred to 10 mL of water or surfactant to create an *ca.* 6 μM solution. In order to avoid changes in the absorption spectrum due to further aggregation, the aggregate solutions were used immediately after preparation. Photostability and/or fluorescence experiments of **AV** in surfactants (CTAB, TTAB, SDBS, SL and in SDS) above their respective critical micelle concentration (CMC) values were performed 24 hours post-creation to ensure that the molecule partitioned into the micelles.

Photostability studies. Solar simulated UV radiation was generated by a solar simulator (Model 16S, 150 W, Solar Light Company, Glenside, PA). The spectral output travelled through an optical fiber to a 1cm pathlength quartz cuvette. The fiber was placed in front of the cuvette such that the UV output beam incident on the sample had a diameter of 1 cm. The UV spectrum was composed of 30 mW UVA and 1 mW UVB, which is excellent agreement with the UVA:UVB ratio of the standard solar spectrum ASTM G173-03.[37] The concentration of **AV** was *ca.* 6 □M in all solvents, corresponding to a peak optical density < 0.2, to prevent inner-filter effects. Each solution had an identical volume (3.2 mL) and was stirred constantly during irradiation. The solar simulator dose control system was used to set the UV dose at time (*t*)=0, 60, 300, 600, 1200, and 2400 (+/- 0.2 seconds), where 56 s is equivalent to 1 minimal erythemal dose measured as 22 mJ cm^{-2} UVB, and 660 mJ cm^{-2} UVA. Absorption spectra were recorded at each time point by a Cary-500 absorption spectrophotometer. Experiments were performed in duplicate. Absorption

spectra of the neat solvents were recorded and showed no absorption > 250 nm; they were subtracted from the sample spectra. In order to determine the fraction of enol (f_{Enol}) remaining after irradiation period, each absorption spectrum was normalized by dividing by the absorbance at the enol peak (λ_{max} which varies between 350 and 400 nm depending on solvent) of the *t*=0 spectrum:

$$f_{Enol}(t) = \frac{Abs(\lambda_{max},t)}{Abs(\lambda_{max},t=0)} \quad (1)$$

where $Abs(\lambda_{max},t)$ is the absorbance at the λ_{max} of the enol peak at *t*=60, 300, 600, 1200 or 2400 s and $Abs(\lambda_{max},t=0)$ is the absorbance at *t*=0 s.

Fluorescence: Steady-state and anisotropy spectra. Fluorescence spectra of dilute solutions and colloidal suspensions were acquired using a QuantaMaster 8000 (Horiba, Irvine, CA). All samples were stirred during each experiment. The excitation anisotropy (*r*) spectra were calculated using equation 2

$$r = \frac{I_{\parallel} - I_{\perp}}{I_{\parallel} + 2I_{\perp}} \quad (2)$$

where the emission polarizer is parallel ($I_{\parallel}$) or perpendicular ($I_{\perp}$) to the excitation polarizer.[38]

Time-resolved fluorescence. Dilute solutions were used to collect fluorescence lifetime (τ_{fl}) data. The excitation wavelength at 320 nm was generated by pumping an OPA (Palitra, Quantronix) with 800 nm, 150 fs pulses from a Ti:sapphire regenerative amplifier (1 kHz, Libra, Coherent). The laser power was set to be at or below 75 μW at the sample surface. Fluorescence lifetime data were collected using a front face geometry with a picosecond streak camera (Streakscope, Hamamatsu C4334) whose instrument response function had a full-width-half maximum of ~25

ps. Scattered IR and UV light were removed by placing two 420 nm long wave pass filters and a hot mirror before the input of the streak camera.

Results and Discussion

The characteristic **AV** $\pi - \pi^*$ transition in the UVA shifts to longer wavelengths with increasing solvent polarity (Supporting Information, Figure S1). In non-aqueous, non-polar cyclohexane, the enol absorption peaks at 352 nm, but is shifted in polar, aprotic solvents like ethylene glycol where the λ_{max} is 362 nm (Table 1). These results are consistent with the literature and illustrate how the polar nature of the first excited singlet state (S_1) is stabilized by polar solvents lowering the S_0-S_1 the energy gap.[20, 39]

In contrast to organic solvents, **AV** is effectively insoluble in water. It forms aggregates as indicated by a faintly cloudy solution that yields the typical scattering profile from a colloidal suspension, with an exponential tail that extends to longer wavelengths (Supporting Information, Figure S1). These results are similar to those of the UVB filter octylmethoxycinnamte.[36] This spectrum also exhibits clear signs of aggregation, with a strong broadening and redshift of the lowest energy absorption peak. The change in the absorption lineshape is consistent with a disordered solid in which J-type (leading to an absorption red-shift) aggregates exist.[40]

The insolubility of **AV** in neat H_2O motivated us to use the surfactant SDS as an alternative way to expose **AV** to H_2O molecules while preventing aggregation. Absorption spectral data show that aggregation of **AV** depends on the concentration of SDS in the solution (Figure 1). At concentrations below the SDS CMC (8 mM), the absorption profile is similar to that of colloidal

AV, with a broadening of the absorption spectrum as well as a baseline offset due to scattering. But as the SDS concentration increases above the CMC, there is a sudden increase in the absorbance accompanied by a narrowing of the absorption, so that it resembles the fully solubilized **AV** in non-aqueous solutions.

To gain a better understanding of the molecule's incorporation into the micelle, data from steady-state and time-resolved fluorescence measurements were analyzed. The normalized fluorescence spectra of **AV** in several different solvents, including the aggregated form in neat H_2O (0 mM SDS), are shown in Figure 2. As with the absorption spectra, there is a systematic red shift as the solvent polarity is increased. In contrast to the spectra in organic solvents, the spectrum of the aggregates in water is very broad, with the peak at 430 nm followed by large shoulder at 530 nm. The shoulder at 530 nm disappears as the concentration of SDS in water increases above the CMC (Supporting Information, Figure S2) and is completely absent in 20 mM SDS. The loss of this shoulder is consistent with the assumption that it reflects an aggregated form of **AV** rather than the molecular emission, which appears only at SDS concentrations above the CMC. **AV** is not a strongly emissive species, which is consistent with its ability to return to the ground state via internal conversion on a sub-nanosecond timescale.[30] While this rapid internal conversion is useful for it to fulfill its function as a UV filter, it makes measurement of the fluorescence spectrum challenging, especially in non-polar solvents like cyclohexane. Because of the low signal levels, we could not reliably measure absolute quantum yields. We could determine the relative fluorescence intensity increase in more polar solvents, with **AV** emitting ~6x more in methanol than in cyclohexane and ~10x more in 20 mM SDS than in methanol (Supporting Information, Figure S3).

Both absorption and fluorescence data suggest that once the micelles are formed, the **AV** molecules de-aggregates. Presumably it is incorporated into the SDS micelle. Given that the micelle interior is composed of hydrophobic alkyl chains, one would expect that if **AV** was encapsulated fully within the hydrophobic core, then the absorption and emission shifts would be similar to those of cyclohexane (λ_{max} = 352 nm, Table 1). Instead, the absorption (Figure S1, Table 1) and fluorescence (Figure 2, Table 1) shifts of **AV** in SDS micelles are similar to those in polar, protic solvents, indicating that the molecule resides in an environment even more polar than that provided by methanol or ethylene glycol.

The question of whether **AV** resides in the micelle can be addressed by steady-state anisotropy experiments. The interior of the micelle tends to isolate the molecules in more viscous surroundings, preventing depolarization due to energy migration and rotation diffusion. Figure 3a shows that in 20 mM SDS the anisotropy is well-behaved with a single value across the first absorption band. This spectrally flat anisotropy value was observed in all solvents (Supporting Information, Figure S4). The anisotropy undergoes a sudden increase at the CMC of SDS (8 mM) (Figure 3b), similar to the jump in absorption intensity seen in Figure 2. Below the CMC, the anisotropy of the aggregated form in water is low (*r*=0.15), which we attribute to intermolecular energy transfer within the aggregate that depolarizes the fluorescence.[41-43] Above the CMC, the anisotropy peaks at *r*=0.35 (20 mM SDS) similar to that measured in methanol (*r*=0.32), and to values reported for other dyes in micelles.[44] These higher anisotropy values likely reflect the fact that the transition dipole orientation in micelles and methanol can only be randomized by molecular rotation. The rotational diffusion time of **AV** has not been measured, but typical values for small aromatic molecules are in the range of 10-50 ps in pure liquids, as

compared to its fluorescence lifetime of less than 20 ps.[45] These timescales are comparable, and the steady-state anisotropy depends on their ratio (Supporting Information). There are several additional factors that can slow rotational diffusion in the micelles and in methanol and give rise to higher steady-state anisotropies. One is the hindered environment leading to higher anisotropy values for small molecules in the SDS micelle.[44] A second is the association of hydrogen-bonded solvent molecules to the solute, as in the work by Das *et al.* showing that intermolecular hydrogen bonding between 3-hydroxyflavone and protic solvents slows down rotational diffusion and leads to higher fluorescence anisotropy values.[46] Taken together, the spectral shifts and anisotropy changes are both consistent with **AV** being successfully encapsulated inside the SDS micelles and sequestered near the headgroup-water interface rather than the hydrophobic core.

Time-resolved fluorescence lifetime measurements also support the idea that **AV** exists in a polar environment in the SDS micelle. The increased fluorescence yield in methanol and 20 mM SDS suggested that the fluorescence lifetime has increased due to slower internal conversion. To confirm this, we used a picosecond streak camera to measure **AV**'s fluorescence decay after excitation at 370 nm. In methanol, the signal decayed within the instrument response function of our system (< 7ps), and we observed a very weak longer-lived nanosecond decay at < 1% of the total signal amplitude (Figure 4). We could not rule out that this emission was the result of an impurity, so we did not analyze it further. In contrast, the fluorescence decay (τ_f) of the 20 mM SDS sample could be resolved (Figure 4) and exhibited bi-exponential behavior reflecting two emitting species and was fit to the function $A_1 e^{-t/\tau_1} + A_2 e^{-t/\tau_2}$. Convolution with the instrument response yielded a dominant species (A_1=0.9) with τ_1=18 ps and a second longer lived

species with a smaller amplitude (A_2=0.1) with τ_2=125 ps. The integrated fluorescence signal from a biexponential decay is proportional to its average weighted lifetime given by $A_1\tau_1 + A_2\tau_2$ = 28.7 ps for **AV** in SDS micelles. Given the fact that **AV**'s fluorescence yield is 10-60× greater in SDS micelles than in methanol and cyclohexane, respectively, this result implies that the excited state lifetime in those solvents should be ≤ 3 ps, in good agreement with femtosecond transient absorption results.[30] Both our steady-state and time-resolved measurements suggest that **AV**'s excited state lifetime is significantly extended in SDS micelles, most likely due to a polar local environment. This stabilization in polar solvents was inferred from transient absorption experiments and is also consistent with the observation that the internal conversion rate of dibenzoylmethane **(DBM**), an **AV** analog, slowed down in more polar solvents.[30, 47, 48] They hypothesized that a U-shaped complex between the **DBM** keto-enol and hydrogen bonding solvents can enhance the rigidity of the molecule, reducing the likelihood of energy dissipation through rotational pathways. Intermolecular hydrogen bonding also helps reconcile the high anisotropy and longer lifetime values experienced by **AV** in micelles (Supporting Information).

The preceding results have shown that **AV**'s photophysics are quite sensitive to its environment, although its UVA absorption is always present. From a practical standpoint, because of its worldwide use in sunscreens, it is an interesting question whether the different solvent environments also affect the long-term photostability of **AV**. As described in the Introduction, the first step in the loss of UVA protection is the formation of the diketone isomer with a characteristic absorption peak *ca.* 270 nm. In non-polar cyclohexane, solar UV irradiation leads to rapid loss of the keto-enol absorption at 352 nm and growth of the diketone peak at 270 nm (Figure 5a). The presence of an isosbestic point at 295 nm is consistent with a simple two-

state tautomerization. In cyclohexane, **AV** undergoes almost complete tautomerization to the diketone structure (f_{Enol}=0.03 at 1200 s (Table 1)), consistent with the results of Mturi *et al*.[20] In aqueous colloidal suspensions, tautomerization also dominates the change in absorption of the molecule where the isosbestic point at 310 nm identifies the change in molecular structure from the UVA absorbing enol to the UVC absorbing diketone (Figure 5b). In both of these samples, there is an absence of intermolecular hydrogen bonding opportunities due to a local environment composed of either cyclohexane molecules or other **AV** molecules. However, when we switched to methanol, the absorption spectrum of **AV** changed only by ~1% under solar-simulated UV irradiation up to 1200 s (Figure 5c), which is also consistent with the literature.[17-22] However, interestingly, **AV** showed a similar level of stability in 20 mM SDS (Figure 5d), losing only 4% of its initial absorbance at 356 nm.

The role of micellar encapsulation in stabilizing **AV** can be seen in Figure 6a, which shows the fraction of the enol absorbance at 356 nm remaining (f_{Enol}) after 1200 s of UV irradiation, for different SDS concentrations. In neat water (0 mM SDS), **AV** rapidly degrades in aggregate particles and f_{Enol}=0.03. As the concentration of SDS is increased, f_{Enol} increases as well, approaching 1.0 at SDS concentrations above the CMC. To achieve maximum stability, the concentration of SDS must be above the CMC to fully separate the **AV** molecules while allowing access to H_2O molecules. We found that the ability of a surfactant to stabilize **AV** also depends on its chemical structure. While SDS was the most effective at preserving the enol form, other surfactants also showed varying degrees of photostabilization of **AV**. Figure 6b shows the initial decay of the **AV** absorbance in surfactants SDS, CTAB, SL, and TTAB. Interestingly, **AV** in CTAB undergoes the most rapid decay. These results suggest that encapsulation of **AV** inside a micelle

is not enough to prevent diketonization, and that the surfactant chemical structure or micelle shape also plays a role. Presumably the presence of labile hydrogen donors is required to facilitate intramolecular chelate recovery. This observation may help explain why encapsulation of **AV** in hydroxypropyl-b-cyclodextrin also improved its photostability.[49]

The ability of polar, protic solvents to prevent diketonization has been observed for other keto-enol systems. Tobita and coworkers postulated a mechanism for **DBM** by which an intermolecular hydrogen bond acts as an intermediate to catalyze the reformation of the intramolecular chelate, allowing the process to compete more effectively with the diketone tautomerization pathway.[47] In this model, the presence of even a few H_2O molecules inside the micelle may be sufficient to reform the chelate. We tested this hypothesis by performing the photostability experiment using polar, aprotic acetonitrile under both wet and dry conditions. We found that in the presence of 1% water, 85% of the enol absorption remains after 2400 s of solar simulated UV irradiation (Supporting Information, Figure S5a). Additionally, there was no clear isosbestic point in the spectra, indicating that photodegradation may be occurring through pathways different than tautomerization. In contrast, a clear isosbestic point and dramatic decrease in the enol portion of the absorption spectra of **AV** is detected in dry acetonitrile (Supporting Information, Figure S5b). These data suggest that it is the ability of the micelle to allow H_2O molecules to access isolated **AV** molecules that leads to enhanced photostability.

It is interesting to compare **AV** with curcumin, another well-studied keto-enol molecule, where micellar encapsulation leads to enhanced stability. Curcumin undergoes a ground state hydrolysis of the enol, and micellar encapsulation protects the molecule from the surrounding water.[50-53] We found that **AV** slowly undergoes hydrolysis in SDS solutions below the CMC, with

the decrease occurring over a period of 24 hours (Supporting Information, Figure S6). Above the CMC, the **AV** absorption remained stable indefinitely in the absence of light. As with curcumin, the micelles appear to protect **AV** from water hydrolysis. In SDS micelles, we appear to have a balanced situation in which specific interactions with H_2O can suppress **AV** photoketonization, but the H_2O molecules do not have completely free access to the **AV** molecule, which would lead to ground state hydrolysis. In fact, we may be able to draw an analogy to the photophysics of curcumin, where it is proposed that it is the access to water that facilitates excited state proton transfer within 50-80 ps in micelles and within 21 ps in cyclodextrin systems.[50, 54] Rapid excited state proton transfer in turn allows for the stabilization of the enol structure. Although the detailed ground state (**AV**) and excited state (curcumin) proton transfer pathways remain to be elucidated, in both molecules the presence of a hydrogen bonding partner appears to play a key role for increasing their photostability in micelles.

Conclusion

The results in this paper clarify how **AV**, the only UV filter approved by FDA to absorb UVA radiation, undergoes photodegradation. **AV** is highly susceptible to diketonization in both nonpolar solvents and in its aggregated form but is considerably more stable in polar, protic solvents like methanol. By studying its stability in different surfactant solutions, we show that incorporation of **AV** into SDS micelles can achieve stability levels comparable to neat methanol. Steady-state spectral shifts, fluorescence anisotropy, and time-resolved fluorescence decay measurements are all consistent with **AV** experiencing a polar environment after encapsulation. We propose that **AV** is encapsulated in the palisade layer of the SDS micelles, which allows access

to water molecules that facilitate the re-formation of the enol form after photon absorption and relaxation. Although the detailed mechanism of **AV** tautomerization remains unclear, this work suggests that a microheterogeneous strategy might be a fruitful approach to make improved sunscreens with stable UVA blocking capability. The advantage of the micellar systems is that they can be adapted to formulations that are required for practical sunscreens. An improved understanding of the role of proton transfer in microheterogeneous systems may provide a route to more stable and effective sunscreens.

Acknowledgements

This research was supported by the National Science Foundation grants DMR-1810514.

Table 1. Steady-state and Time-Resolved Spectroscopic Parameters of Avobenzone in Different Solvent Conditions

Solvent	Absorption λ_{max} (nm)	Emission λ_{max} (nm)	f_{Enol}[1] (std dev)	τ_{fl} (ps)
Cyclohexane	352	402	0.03 (0.01)	< 7
Methanol	360	410	0.99 (0.00)	< 7
Ethylene Glycol	362	414	0.96 (0.00)	--
Water	368	423	0.35 (0.02)	--
SDS (20 mM)	363	419	0.96 (0.01)	18 ps (a = 0.9) 125 ps (a = 0.1)
SDS (15 mM)	363	417	0.97 (0.01)	--
SDS (12 mM)	363	419	0.96 (0.00)	--
SDS (10 mM)	363	419	0.94 (0.01)	--
SDS (8mM)	363	421	0.81 (0.06)	--
SDS (6 mM)	363	424	0.87 (0.02)	--
SDS (4 mM)	401	422	0.79 (0.19)	--
SDS (2 mM)	363	424	0.67 (0.17)	--
CTAB (2 mM)	356	--	0.82 (0.02)	--
SDBS (5 mM)	361	--	0.96 (0.02)	--
SL (42 mM)	361	--	0.93 (0.01)	--
TTAB (8 mM)	361	--	0.91 (0.04)	--

[1]fraction of enol remaining after 1200 s^{-1} (0.5 J cm^{-2} UVB, 14.1 J cm^{-2} UVA)

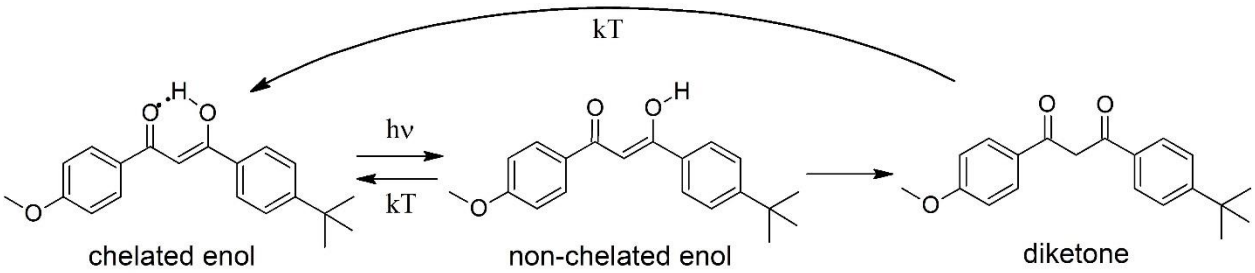

Scheme 1. Examples of the non-chelated and chelated keto-enol and diketone tautomers of avobenzone. Because of the asymmetry of the molecule, the two keto-enol structures also have a counter molecule that is not shown. Additionally, the non-chelated enol may have multiple conformers.[32]

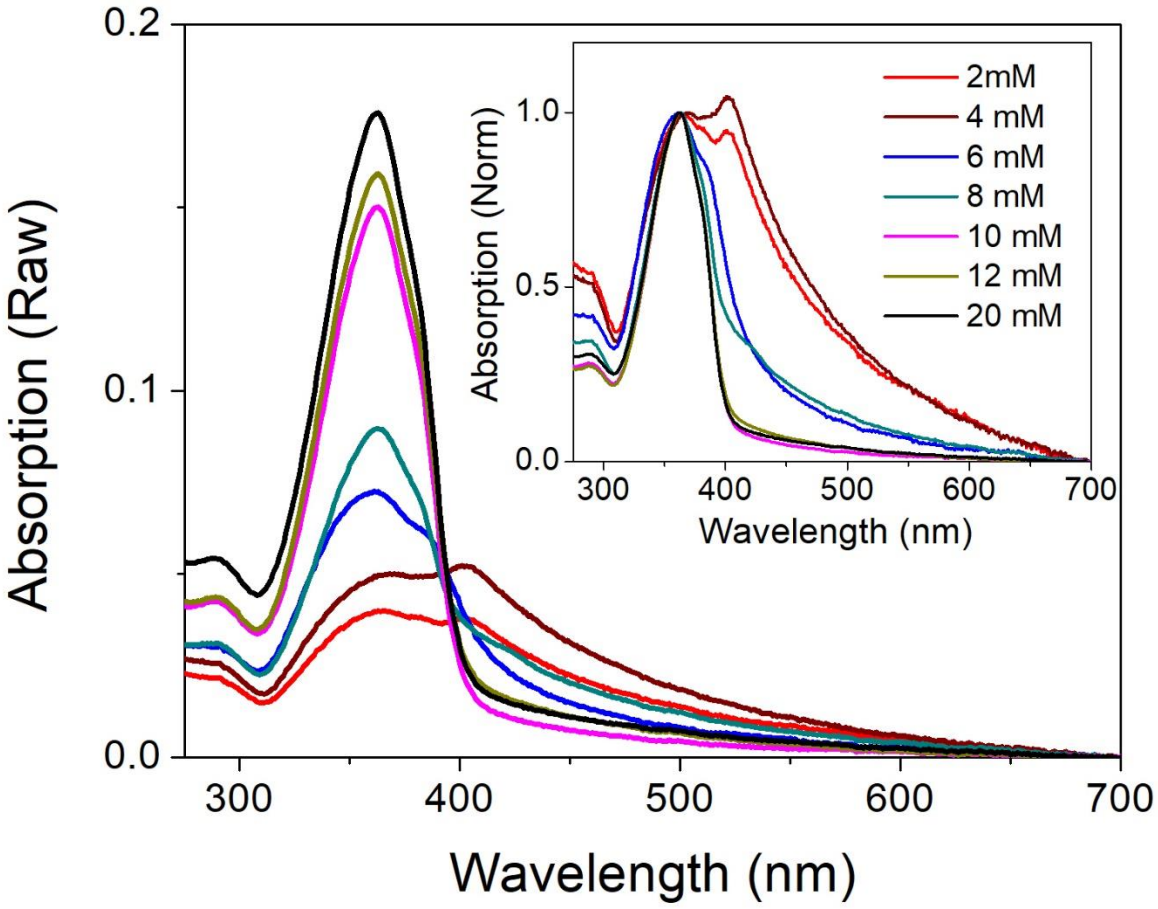

Figure 1. Avobenzone in increasing SDS concentration. Solubility improves with increasing SDS concentration, where the aggregates that broaden the spectrum below the CMC (8 mM) disappear with a concomitant increase in the left shoulder of the enol absorption.

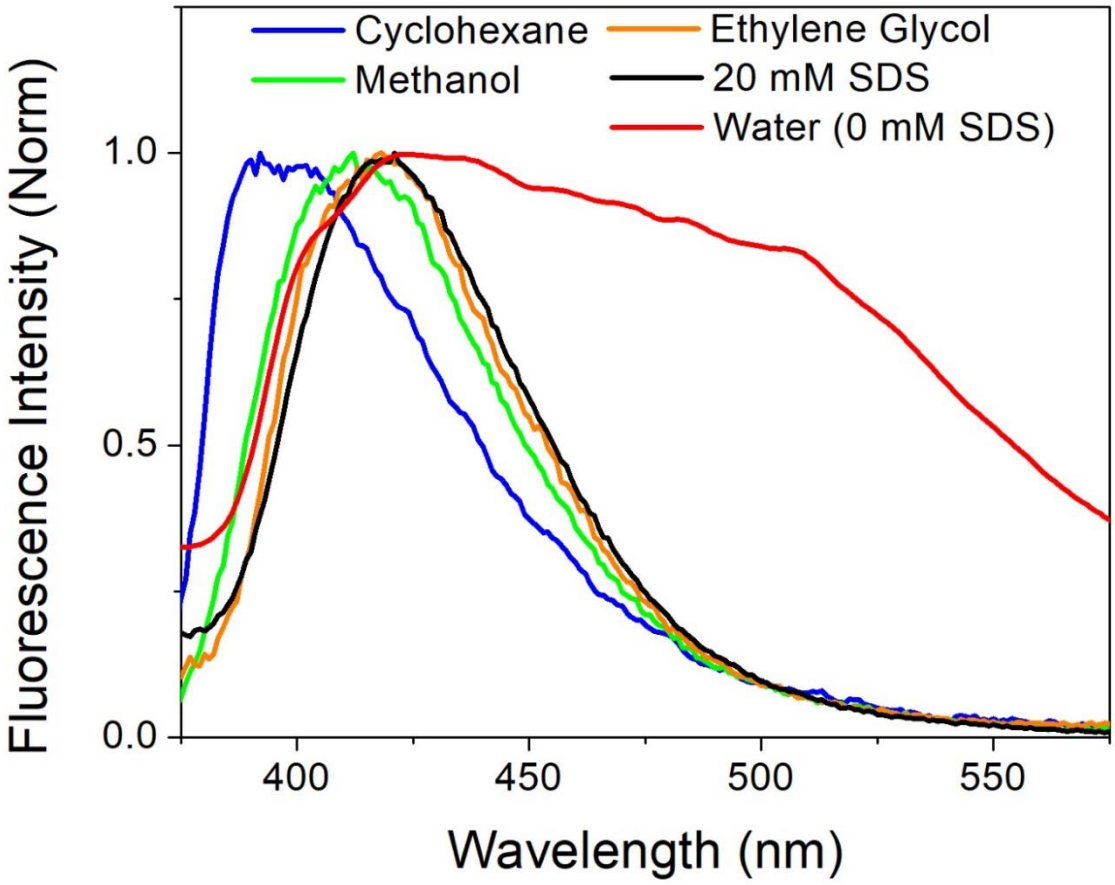

Figure 2. Fluorescence emission spectra of dilute solutions of avobenzone excited at 320 nm in cyclohexane (blue), methanol (green), ethylene glycol (orange), 20 mM SDS (black), and of aggregated colloidal avobenzone in water (0 mM SDS). The spectra shift to the red with increasing dielectric constant (Table 1).

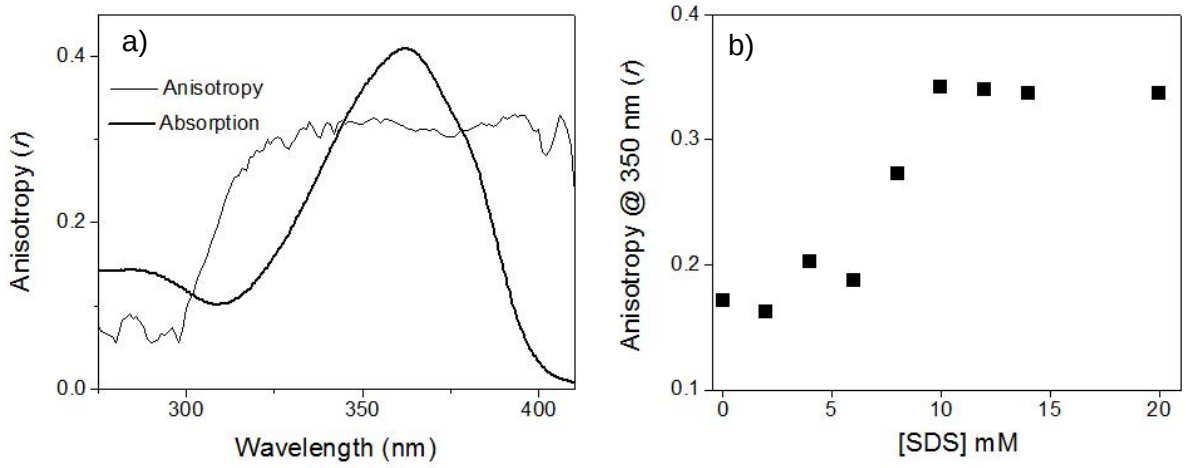

Figure 3. a) The excitation anisotropy spectrum (thin black line) and the absorption spectrum (thick black line) of avobenzone in 20 mM SDS. b) The anisotropy at 350 nm near the λ_{max} of the enol species at different concentrations of SDS. The CMC of SDS is 8 mM, which is at the midpoint of the graph.

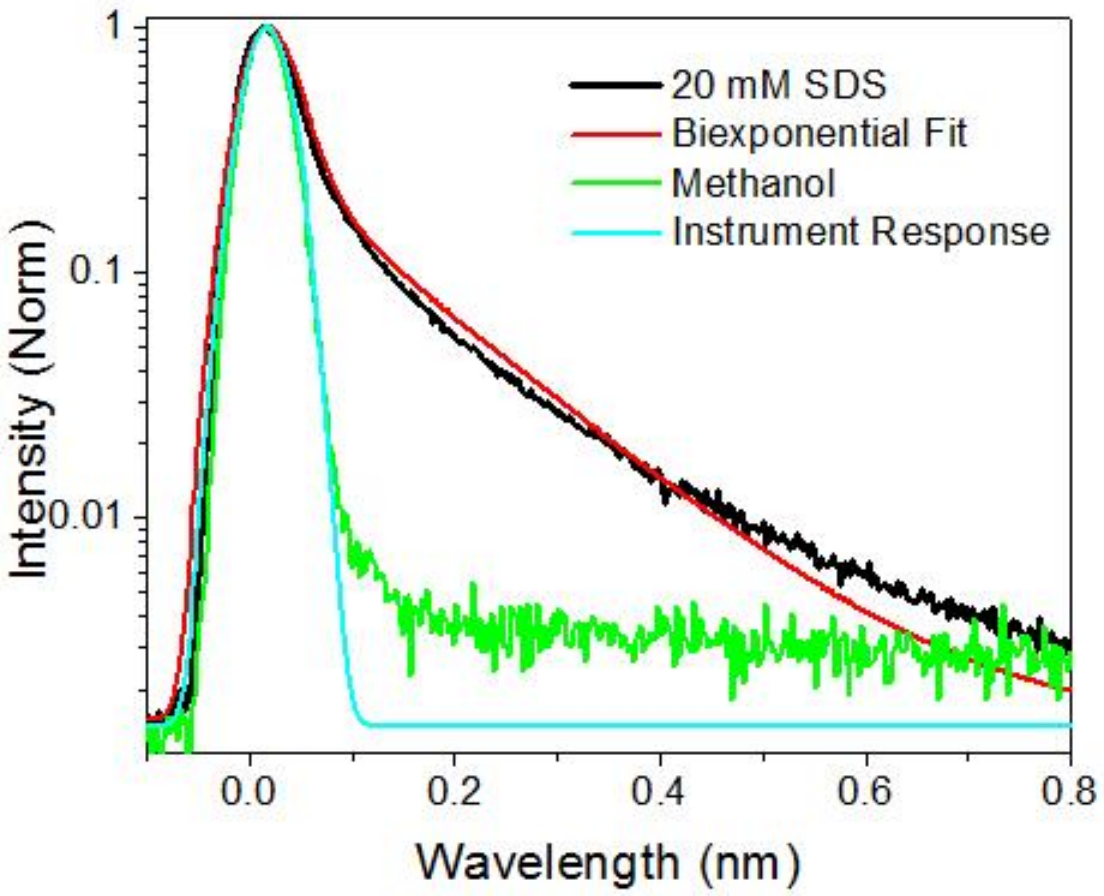

Figure 4. Fluorescence lifetime data of avobenzone in 20 mM SDS (black), which was fit to a biexponential decay (red). Avobenzone in methanol (green) exhibited a lifetime that was within the instrument response (cyan), compared to the longer lived lifetime exhibited in 20 mM SDS.

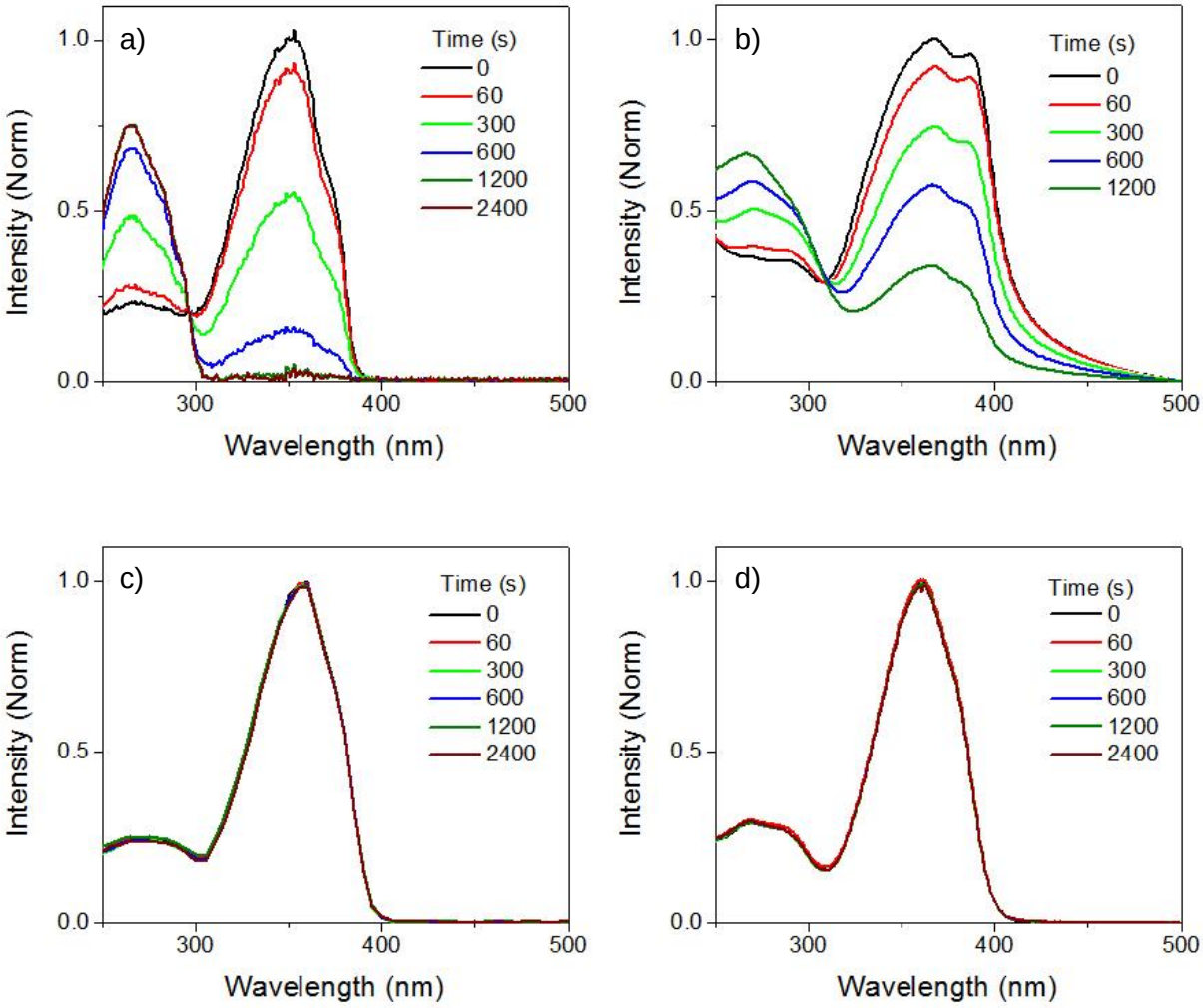

Figure 5. The absorption spectrum of ~6 μM avobenzone in cyclohexane (a), water (b), methanol (c), and 20 mM SDS (d) as a function of solar-simulated UV irradiation time.

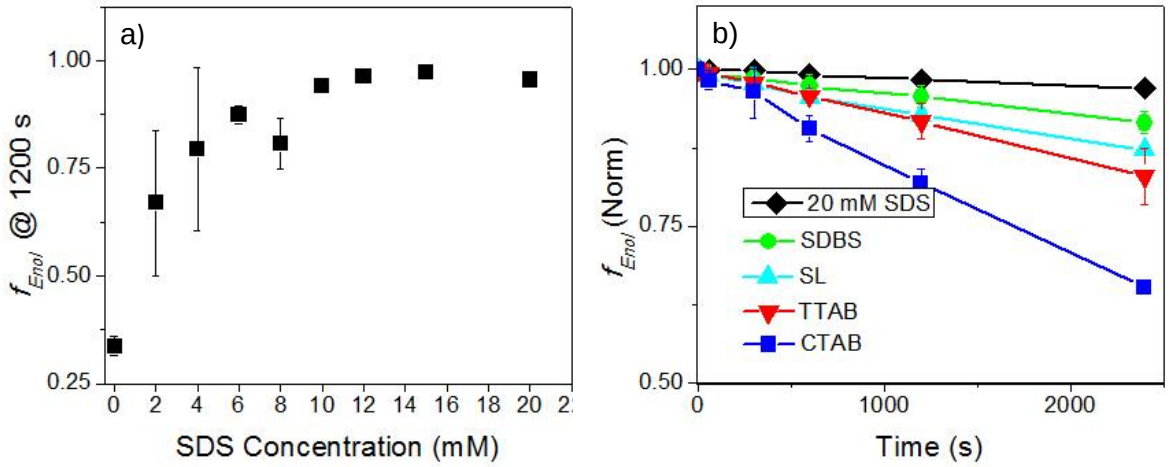

Figure 6. a) The fraction of enol remaining after 1200s of UVA/UVB irradiation at different concentrations of SDS. b) The fraction of enol remaining as a function of irradiation time for micellular solutions of different surfactants.

References

1. S. Amano, Characterization and mechanisms of photoaging-related changes in skin: damages of basement membrane and dermal structures, *Experimental Dermatology*, 2016, **25**, 14-19.
2. J. J. Bernard, R. L. Gallo and J. Krutmann, Photoimmunology: how ultraviolet radiation affects the immune system, *Nature Reviews Immunology*, 2019, **10.1038/s41577-019-0185-9**, ahead of print.
3. P. M. Farr and B. L. Diffey, The erythemal response of human skin to ultraviolet radiation, *The British Journal of Dermatology*, 1985, **113**, 65-76.
4. V. Grandi, P. Di Gennaro, S. Torrigani, L. Basco, I. Lastrucci and N. Pimpinelli, Ingenol mebutate-mediated reduction in p53-positive keratinocytes in skin cancerization field directly correlates with clinical response in patients with multiple actinic keratoses, *Journal of the European Academy of Dermatology and Venereology*, 2019, **33**, 1297-1303.
5. V. T. Natarajan, P. Ganju, A. Ramkumar, R. Grover and R. Gokhale, Multifaceted pathways protect human skin from UV radiation, *Nature Chemical Biology*, 2014, **10**, 542-551.
6. C. Nishigori, Current concept of photocarcinogensis, *Photochemical and Photobiological Sciences*, 2015, **14**, 1713-1721.
7. M. Norval, The mechanisms and consequences of ultraviolet-induced immunosuprresion, *Progress in Biophysics and Molecular Biology*, 2006, **92**, 108-118.
8. L. A. Baker, S. E. Grennough and V. G. Stavros, A perspective on the ultrafast photochemistry of solution-phase sunscreen molecules, *Journal of Physical Chemistry Letters*, 2016, **7**, 4655-4665.
9. C. A. Bonda, in *Sunscreens: Regulation and Commerical Development*, ed. H. A. Shaath, Taylor & Francis, Boca Raton, 2005.
10. B. Diffey, R. P. Stokes, S. Forestier, C. Mazailier and A. Rougier, Suncare product photostability: a key parameter for a more realistic in vitro efficacy evaluation, *European Journal of Dermatology*, 1997, **7**, 226-228.
11. E. L. Holt and V. G. Stavros, Applications of ultrafast spectroscopy to sunscreen development, from first principles to complex mixtures, *International Reviews in Physical Chemistry*, 2019, **38**, 243-285.
12. S. P. Huong, V. Andriew, J.-P. Reynier, E. Rocher and J.-D. Fourneeron, The photoisomerization of the sunscreen ethylhexyl p-methoxy cinnamate and its influence on the sun protection factor, *Journal of Photochemisty and Photobiology A Chemistry*, 2007, **186**, 65-70.
13. R. M. Sayre, J. C. Dowdy, A. J. Gerwig, W. J. Shields and R. V. Lloyd, Unexpected photolysis of the sunscreen octinoxate in the presence of the sunscreen avobenzone, *Photochemistry and Photobiology*, 2005, **81**, 452-456.
14. N. Serpone, A. Salinar, A. V. Emeline, S. Horikoshi, H. Hidaka and J. Zaho, An in vitro systematic spectroscopic examination of the photostabilities of a random set of commercial sunscreen lotions and their chemical UVB/UVA active agents, *Photochemical and Photobiological Sciences*, 2002, **1**, 970-981.
15. R. Stokes and B. Diffey, In vitro assessment of sunscreen photostability: the effect of radiation source, sunscreen application thickness and substrate, *International Journal of Cosmetica Science*, 1999, **21**, 341-351.
16. *Sunscreen Drug Products for Over-the-Counter Use: Final Rule and Proposed Rules*, Food and Drug Administration, Department of Health and Human Services, 2011, **76**, 35620-35665.
17. A. Cantrell and D. J. McGarvey, Photochemical studeis of 4-tert-butyl-4'-methoxydibenzoylmethane (BM-DBM), *Journal of Photochemistry and Photobiology B: Biology*, 2001, **64**, 117-122.

18. D. Dondi, A. Albini and N. Serpone, Interactions between different solar UVB/UVA filters contained in commerical sunscreens and consquent loss of UV protection, *Photochemical and Photobiolical Sciences*, 2006, **5**, 835-843.
19. A. Kikuchi, N. Ogachi and M. Yagi, Optical and electron parametic resonance studies of the excited states of 4-tert-butyl-4'-methoxydibenzoylmethane and 4-ter-butyl-4'-methoxydibenzoylpropane, *Journal of Photochemistry and Photobiology A Chemistry*, 2009, **200**, 1474-1479.
20. G. J. Mturi and B. S. Martinicigh, Photostability of the sunscreening agent 4-tert-butyl-4'-methoxydibenzoylmethane (avobenzone) in solvents of different polarity and proticity, *Journal of Photochemisty and Photobiology A. Chemistry*, 2008, **200**, 410-420.
21. N. M. Roscher, M. K. O. Lindermann, S. B. Kong, C. G. Cho and P. Jiang, Photodecomposition of several compounds commonly used as sunscreen agents, *Journal of Photochemistry and Photobiology A Chemistry*, 1994, **80**, 417-421.
22. W. Schwack and T. Rudolph, Photochemistry of dibenzoyl methane UVA filters Part I, *Journal of Photochemisty and Photobiology B Biology*, 1995, **28**, 229-234.
23. M. P. Kojic, M., Etinski, M., A new insight into the photochemistry of avobenzone in gas phase and acetonitrile from ab initio calculations, *Physical Chemistry Chemical Physics*, 2016, **18**, 22168-22178.
24. G. H. Trossini, V. G. Maltarollo, R. D. A. Garcia, C. A. S. O. Pinto, M. V. R. Velasco, K. M. Honorio and A. R. Baby, Theoretical study of tautomers and photoisomers of avovenzone by DFT methods, *Journal of Molecular Modeling*, 2015, **21**, 319-325.
25. I. Andrae, F. Bohn, A. O. Bringhen, H. Gozenbach, T. Hill, I. Mulroy and T. G. Truscott, *Journal of Photochemistry and Photobiology B: Biology*, 1997, **37**, 147-150.
26. P. Markov and I. Petkov, On the photosensitivity of dibenzoylmethane, benzoylacetone and ethyl benzoylacetate in solution, *Tetrahedron*, 1977, **33**, 1013-1015.
27. M. Dubois, P. Gilard, P. Tiercet, A. Deflandre and M. A. Lefebvre, Photoisomerization of the sunscreen filter PARSOL 1789, *J. Chim. Phys.*, 1998, **95**, 388-394.
28. H. Gozenbach, T. J. Hill and T. G. Truscott, The triplet energy levels of UVA and UVB sunscreens, *Journal of Photochemisty and Photobiology B: Biology*, 1992, **16**, 377-379.
29. C. A. Bonda, A. Pavlovic, K. M. Hanson and C. J. Bardeen, Singlet quenching proves faster is better for photostability, *Cosmetics and Toiletries*, 2010, **125**, 40-48.
30. A. D. Dunkelberger, R. D. Kieda, B. M. Marsh and F. F. Crim, Picosecond dynamics of avobenzone in solution, *Journal of Physical Chemistry A*, 2015, **119**, 6155-6161.
31. C. A. Bonda, P. Marinelli, P. Trivedi, S. Hopper and G. Wentworth, Avobenzone photostability in simple polar and non-polar solvent systems., *Journal of Cosmetic Science*, 1998, **49**, 210-212.
32. A. Deflandre and G. Lang, Photostability assessment of sunscreens-benzylidene camphor and dibenzoylmethane derivatives., *International Journal of Cosmetic Science*, 1988, **10**, 53-62.
33. G. Marti-Mestres, C. Fernandez, N. Parsotam, F. Nielloud, J. P. Mestres and H. HMaillols, Stability of UV filters in different vehicles: solvents and emulusions, *Drug Development and Industrial Pharmacy*, 1997, **23**, 647-655.
34. N. Tarras-Wahlberg, G. Stenhagen, O. Larko, A. Rosen and A. M. Wennberg, Changes in ultraviolet absorption of sunscreens after ultraviolet irradiation., *Journal of Investigative Dermatology*, 1999, **113**, 547-553.
35. V. Vanquerp, C. Rodriguez, C. Coiffard, L. J. M. Coiffard and Y. Roeck-Holtzhauer, High performance liquid chromatogrphic method for the comparison of the photostability of five sunscreen agents., *Journal of Chromatography A*, 1999, **832**, 273-277.

36. K. M. Hanson, S. Narayanan, V. M. Nichols and C. J. Bardeen, Photochemical degradation of the UV filter octyl methoxycinnamate in solution and in aggregates, *Photochemical and Photobiological Sciences*, 2015, **14**, 1607-1616.
37. American Society for Testing and Materials International. ASTM G173-03(2012) Standard Tables for Reference Solar Spectral Irradiance http://www.astm.org/Standards/G173.htm.
38. J. R. Lakowicz, Kluwer Academic/Plenum, New York, Second edn., 1999, pp. 291-366.
39. I. E. Agrapidis-Paloympis, R. A. Nash and N. A. Shaath, *J. Soc. Cosmet. Chem.*, 1987, **38**, 209-221.
40. F. C. Spano, The spectral signatures of Frenkel polarons in H- and J-aggregates, *Accounts of Chemical Research*, 2010, **43**, 429-439.
41. K. M. Gaab and C. J. Bardeen, Wavelength and temperature dependence of the femtosecond pump-probe anisotropies in the conjugated polymer MEH-PPV: Implications for energy-transfer dynamics, *Journal of Physical Chemistry B*, 2004, **108**, 4619-4626.
42. A. Kawski, Excitation energy transfer and its manifestation in isotropic media, *Photochemistry and Photobiology*, 1983, **38**, 487-504.
43. J. R. Lakowicz, *Principles of Fluorescence Spectroscopy*, Kluwer Academic/Plenum, New York, 1999.
44. N. C. Maiti, M. M. G. Krishna, P. J. Britto and N. Periasamy, Fluorescence dynamics of dye probes in micelles, *Journal of Physical Chemistry B*, 1997, **101**, 11051-11060.
45. F. G. R., *Chemical Applications of Ultrafast Spectroscopy*, OXford University Press, New York, 1986.
46. S. Das, S. Ghosh and N. Chattopadhyay, Unprecedented high fluorescence anisotropy in protic solvents: Hydrogen bond induced solvent caging?, *Chemical Physics*, 2016, **644**, 284-287.
47. S. Tobita, J. Ohba, K. Nakagawa and H. Shizuka, Recovery mechanism of the reaction intermediate produced by photoinduced cleavage of the intramolecular hydrogen bond of dibenzoylmethane., *Journal of Photochemistry and Photobiology A Chemistry*, 1995, **92**, 61-67.
48. M. Yamaji and M. Kida, Photothermal tautomerization of a UV sunscreen (4-tert-Butyl-4'-methoxydibenzoylmethane) in acetonitrile studied by steady-state and laser flash photolysis, *Journal of Physical Chemistry A*, 2013, **117**, 1946-1951.
49. J. Yang, C. J. Wiley, D. A. Godwin and L. A. Felton, Influence of hydroxylpropl-B-cyclodextrin on transdermal penetration and photostability of avobenzone., *European Journal of Pharmaceutics and Biopharmaceutics*, 2008, **69**, 605-612.
50. R. Adhikary, P. J. Carlson, T. W. Kee and J. W. Petrich, Excited-state intramolecular hydrogen atom transfer of curcumin in surfactant micelles, *Journal of Physical Chemistry B*, 2010, **114**, 2997-3004.
51. C. Banerjee, S. Ghosh, S. Mandal, J. Kuchlyan, N. J. Kundu and N. Sarkar, Expoloring the photophysics of curcumin in zwitterionic micelar system: an approach to control ESIPT process in the presence of room temperature ionic liquids and anionic surfactant, *Journal of Physical Chemistry B*, 2014, **118**, 3669-3681.
52. M. H. M. Leung and T. W. Kee, Effective stabilization of curcumin by association to plasma proteins: human serum albumin and fibrinogen, *Langmuir*, 2009, **25**, 5773-5777.
53. Y.-J. Wang, M.-H. Pan, A.-L. Cheng, L.-I. Lin, Y.-S. Ho, C.-Y. Hsieh and J.-K. Lin, Stability of curcumin in buffer solutions and characterization of its degradation products., *Journal of Pharmaceutical and Biomedical Analysis*, 1997, **15**, 1867-1876.
54. T. Harada, H. L. McTernan, D.-T. Pham, S. F. Lincoln and T. W. Kee, Femtosecond transient absorption spectroscopy of the medicial agent curcumin in diamide linked γ-cyclodextrin dimers., *Journal of Physical Chemistry B*, 2015, **119**, 2425-2433.

Avobenzone, the only UVA-absorbing molecule approved for use by the FDA, is photolabile degrading to its diketone structure under UV illumination. We have found that photoisomerization is effectively prohibited when avobenzone is sequestered in micelles.

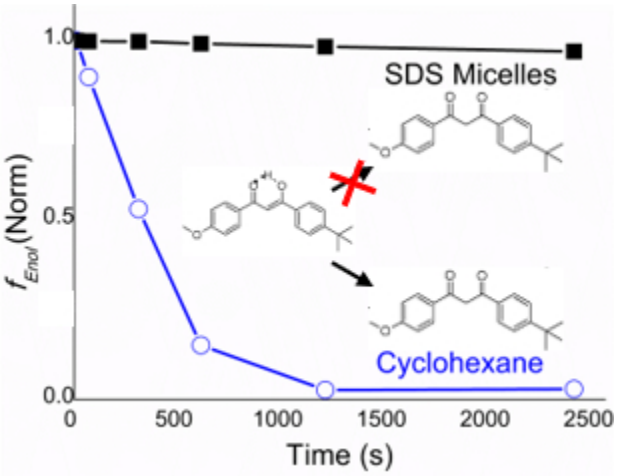

51x39mm (150 x 150 DPI)